
OPTIMAL SURFACE TOPOGRAPHY FOR CELL ADHESION IS DRIVEN BY CELL MEMBRANE MECHANICS

A PREPRINT

Matej Daniel

Faculty of Mechanical Engineering, Czech Technical University in Prague, Czechia
matej.daniel@cvut.cz

Kristin Eleršič Flipič

Faculty of Mechanical Engineering, Czech Technical University in Prague, Czechia

Eva Filová

Institute of Experimental Medicine of the Czech Academy of Sciences, Czechia

Jaroslav Fojt

University of Chemistry and Technology, Prague, Czechia,

July 1, 2020

ABSTRACT

Titanium surface treated with titanium oxide nanotubes was used in many studies to quantify the effect of surface topography on cell fate. However, the predicted optimal diameter of nanotubes considerably differs among studies. We propose a model that explain cell adhesion to nanostructured surface by considering deformation energy of cell protrusions into titanium nanotubes and adhesion to surface. The optimal surface topology is defined as a geometry that gives membrane a minimum energy shape. A dimensionless parameter, the cell interaction index, was proposed to describe interplay between the cell membrane bending, intrinsic curvature and strength of cell adhesion. Model simulation show that optimal nanotube diameter ranging from 20 nm to 100 nm (cell interaction index between 0.2 and 1, respectively) is feasible within certain range of parameters describing adhesion and bending energy. The results indicates a possibility to tune the topology of nanostructural surface in order to enhance proliferation and differentiation of cells mechanically compatible with given surface geometry while suppress the growth of other mechanically incompatible cells.

Keywords titanium; nanotubes; biomechanics; adhesion; surface energy; cell membrane; bending

1 Introduction

Strong bonds between the implant and bone cells [1,2] is required for the long-term stability of the implant in the human body [3]. It was shown that bone cellular response is directly affected by titanium surface characteristics like roughness, chemistry, wettability or more recently studied surface topography [4]. Various methods for surface modification were employed in order to promote cell–substrate interactions [5,6].

The anodic oxidation is adopted to create a nanostructured titanium surface [7] by formation of TiO₂ nanotubular structures (TNTs) [3,8] (Fig. 1A). TNTs increase surface area that favors bone deposition and could improve therapeutic efficiency by serving as a reservoir for drug delivery [9,10]. The advantage of anodic oxidation is that the diameter, the wall thickness and the length of TNTs can be controlled by the process variables such as electrical current power, anodization time, temperature, applied potential, and electrolyte chemical composition [7,11,12]. TNTs length can range from 0.1 up to 1000 μ m while the inner diameter can range from 7 to 150 nm [3,13,14].

Surface treated with TNT array present a controlled environment that allows to quantify the effect of surface topography on cell fate [15]. Nanotube diameter, rather than the other characteristics of the surface layer, exhibits critical impact on cell adhesion and proliferation [8, 9, 16–18]. It was further suggested that there exists an optimal diameter for TNTs that enhance osteointegration [19]. However, estimated values of the optimal diameter are contradictory. Park et al., 2017 [16] reported the optimal nanotube diameter to be 15 nm based on mesenchymal stem cell proliferation on TNT surface. They also report that the cell adhesion and spreading decreases on TNT layers with a tube diameter larger than 50 nm. Yu et al., 2010 [20] found that MC3T3-E1 preosteoblast adheres well on TNTs of diameter 20–70 nm while the cell attachment is low on TNTs of diameter 100–120 nm. Similar behavior was observed for oestoblast-like MG-63 cells that exhibit higher spreading on 30 nm TNTs whereas the larger diameter of 90 nm had the worst cell viability [9]. Both glioma and osteosarcoma cells exhibit optimal cell adhesion, migration, and proliferation on 20 nm TNTs [18]. Limited spreading on larger diameter TNTs was also reported for malignant cancer cells (T24) of urothelial origin [2]. Osteogenic differentiation of primary rat osteoblasts was observed on 35 nm (amorphous phase) and 41 nm (anatase phase) surface [21]. Das et al., 2009 [22] found 2–3 fold increase in human osteoblast attachment and spreading on 50 nm-diameter TNTs surfaces in comparison to flat Ti samples. Oh et al. reported improved adhesion of hMSC on 30 nm TiO₂ nanotubes and improved osteogenic differentiation on nanotubes with a diameter of 70 and 100 nm [23, 24]. MC3T3-E1 osteoblast cells accelerates in the growth on 70 nm TNTs [25]. Brammer et al, 2009 [26] proposed that bone-forming ability of osteoblasts is higher if grown on TNTs of 100 nm diameter. Also Filova et al, 2015 [27] and Voltrova et al, 2019 [28] concludes that optimal diameter of TNTs is around 70 nm for Saos-2 osteoblast-like cell (Fig. 1B).

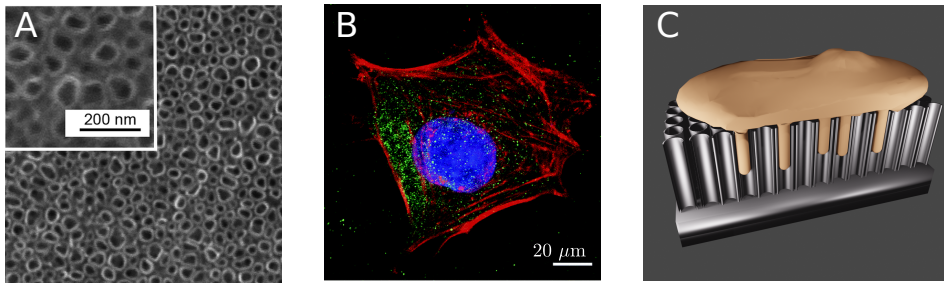


Figure 1: (A) Titanium nanotubes on cpTi of average diameter 66 ± 17 nm and length 1097 ± 75 nm. (B) Immunofluorescence staining of talin in human Saos-2 osteoblast-like cells on nanostructured surface. (C) Schematic view of cell anochored into nanostructured surface. A,B adopted from Voltrova et al, 2019. [28]

The divergence in results could be either caused by variations in surface topography and chemistry, due to individual fabrication protocols or by methods to assess cellular activities [29]. It is also likely, that the type of cell line affect optimal TNT's diameter [19]. While the preference of cells to small diameter TNTs (up to 30 nm) could be explained by integrins packing [16, 30], mechanism of adherence to large diameter has not been explained yet. It was suggested that migration of the cell membrane inside the crystalline nanotubes could be crucial for strong attachment [3, 4, 31]. The cell protrusions into nanotubes could strengthen the adhesive interaction of cells with the surface, and thereby potentially trigger cellular cascades that regulate cell behavior and differentiation [31]. Cell protrusion into TNTs increases contact area for attachment but requires extensive membrane deformation into tubular like structure (Fig. 1C). The aim of the present study is to quantify the overall energy cost of formation of cell protrusion into TNT. The hypothesis based on the experimental results is, that there exist an optimal diameter given by minimum of membrane protrusion energy.

2 Methods

The membrane protrusion into hollow nanotubular structure is assumed to be axisymmetric and its dimensions are determined by the shape of the nanotube. The membrane therefore forms a hollow cylinder of diameter d closed by a hemispherical cup and joined to the central body along the contour shown in Fig. 2. Two energy contribution are considered in mechanics of nanotubular protrusion: the adhesion energy F_a between the TNT inner surface and membrane and the deformation energy F_b of the cell membrane [32].

The adhesion energy is defined as the excess energy released after the cell attaches to the surface [1]. Surface energy quantifies the formation of intermolecular bonds and depends on the contact area A with a proportionality constant γ . According to our model (Fig. 2), the cell membrane is in contact with the TNT only in its central tubular segment (II). The adhesion energy could therefore be expressed as

$$F_a = -\gamma\pi dl \quad (1)$$

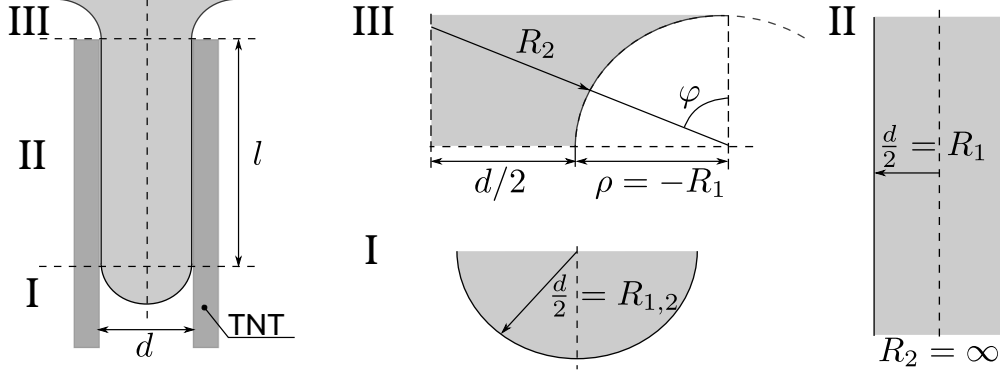


Figure 2: Parametrization of membrane protrusion into TiO_2 nanotubule of diameter d . The shape is divided into three parts: (I) the spherical cup of radius $d/2$, (II) the cylindrical segment of length l and radius $d/2$ and (III) the axisymmetrical collar. Principal curvature R_1 and R_2 are depicted in individual segments.

where the minus sign denotes energy release after adhesion.

Formation of protrusion requires deformation of the membrane from the mostly planar shape into the shape of thin cylinder. The bending energy of the membrane is commonly described by Helfrich energy [33]. The elastic strain energy proposed by Helfrich depends on the mean (H) and Gaussian curvature. As we do not expect the change in cell topology by protrusion formation, the Gauss term could be neglected because of Gauss-Bonnet theorem [34].

$$F_b = \frac{1}{2} k_b \int_A (2H - C_0) dA \quad (2)$$

where k_b is the bending modulus of cell membrane and C_0 is the spontaneous curvature. Spontaneous curvature, or more precisely the spontaneous mean curvature, present a penalty for the mean curvature asymmetry [35]. The mean curvature can be expressed as an average of principal curvature values C_1 and C_2 defined as the inverse values of corresponding radii of curvatures R_1 and R_2 , respectively (Appendix A).

In order to get insight into the interaction between bending and adhesion, we will analyze equilibrium of part II in Fig. 2. Contribution of part I and III could be neglected if the length of the cylinder l is much greater than the diameter, i.e. $l \gg d$. The free energy is expressed from Eqs. (1) and (8).

$$F = \frac{1}{2} k_b \pi l \left(\frac{4}{d} - 4C_0 + C_0^2 d \right) - l\gamma\pi d \quad (3)$$

The central assumption is, that the membrane attains a shape that minimizes the overall energy. We may further assume, that there exist an optimal diameter that corresponds to energy minimum. The minimum of the energy present a stationary point and could be expressed using interior extremum theorem.

$$d_0 = \sqrt{\frac{4k_b}{k_b C_0^2 - 2\gamma}} \quad (4)$$

The value of optimal diameter depends on adhesion constant and bending rigidity of the membrane. The optimal diameter exists if intrinsic curvature is higher than a threshold value. We denote this value as a critical curvature C_{crit} .

$$C_{\text{crit}} = \sqrt{\frac{2\gamma}{k_b}} \quad (5)$$

To describe interaction between the cell protrusions and nanostructured surface, we define a dimensionless number I_c denoted as cell interaction index.

$$I_c = \frac{C_{\text{crit}}}{C_0} \quad (6)$$

As shown above, the energy of cell membrane TNT interaction depends on mechanical properties of membrane described by the bending modulus k_b and the spontaneous curvature C_0 and on interaction between membrane and TNT surface described by density of surface energy γ . The bending modulus of the cell range from $5 k_B T$ for phospholipid

membrane [36] to $200 k_B T$ for cells [37], where k_B is the Boltzmann constant. In the previous study of osteoblasts mechanics, the value of $100 k_B T$ was used to describe osteoblasts bending rigidity [30]. The cell binding energy per unit area γ may range from 0.05 to 56 mJ m^{-2} for various cell types [38]. The spontaneous curvature of the cell membrane is determined by lipid composition and interactions between lipids and proteins [39]. It could have either positive values (intrinsic bending inwards) or negative values (bending outwards). It was reported that lipid bilayer spontaneous curvatures ranges from -0.2 to 0.2 nm^{-1} [40].

3 Results

The existence of optimal diameter of cell for attachment into TNTs depends on the difference between the spontaneous C_0 and the critical curvature. If C_0 is lower than C_{crit} , there is no optimal diameter and cells migrate into TNTs larger than threshold. However, if C_0 is higher than C_{crit} , there exists a limited range of TNTs' diameters in which the formation of membrane protrusion is energetically convenient (Fig. 3C,D). For higher spontaneous curvature, the TNTs' optimal diameter range is smaller and the energy rises considerably for larger diameters (Fig. 3D).

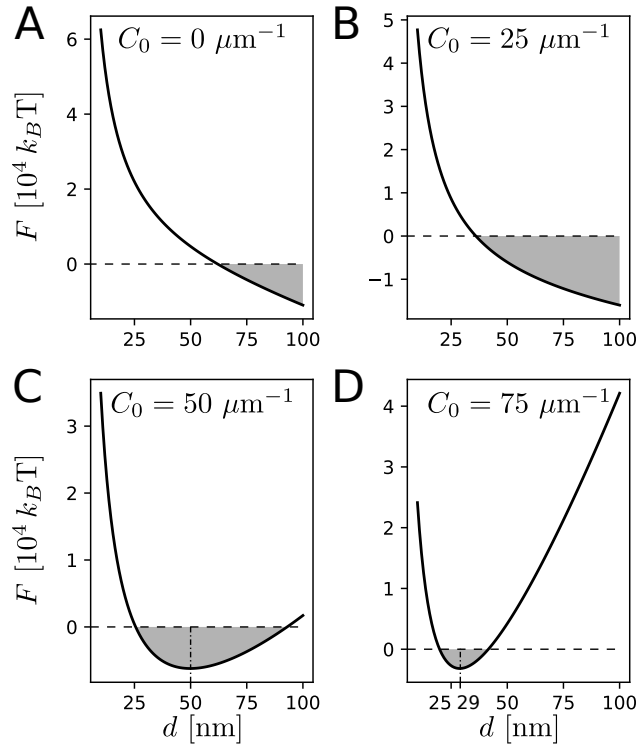


Figure 3: Free energy of membrane protrusion (F) into TNT: (A,B) spontaneous curvature C_0 is lower than the critical curvature C_{crit} , (C,D) spontaneous curvature C_0 is higher than the critical curvature C_{crit} . Gray region indicate area where formation of protrusion is energetically favorable. The critical curvature $C_{\text{crit}} = 35 \mu\text{m}^{-1}$ and energy is calculated for $k_b = 100 k_B T$, $\gamma = 0.25 \text{ mJ m}^{-2}$, $l = 1000 \text{ nm}$ for protrusion shape shown in Fig. 1.

The critical curvature is a function of binding energy per unit area γ and bending stiffness of membrane k_b (Eq. (5)). Increase in adhesion strength (Fig. 4A) and decrease in bending stiffness (Fig. 4B) enhance formation of cylindrical protrusion by lowering membrane free energy. For stiff membrane or limited adhesion between the cell membrane and the TNTs' wall, the migration of membrane into TNTs' is not likely to happen spontaneously (Fig. 4A,B).

Figure 5 shows the dependence of the optimal diameter of TNT (d_0) on the cell interaction index I_c , Eq. (6). For small values of I_c , the contact between nanostructured surface and cell will not be formed as the energy required to bend the membrane is higher than the energy gained in forming adhesion bonds. For I_c between 0.2 and 1, the optimal topology exists and it depends on the spontaneous curvature. Cells with high spontaneous curvature will prefer smaller diameter of TNTs. If I_c is higher than one, the cell will prefer smooth surface against curved one.

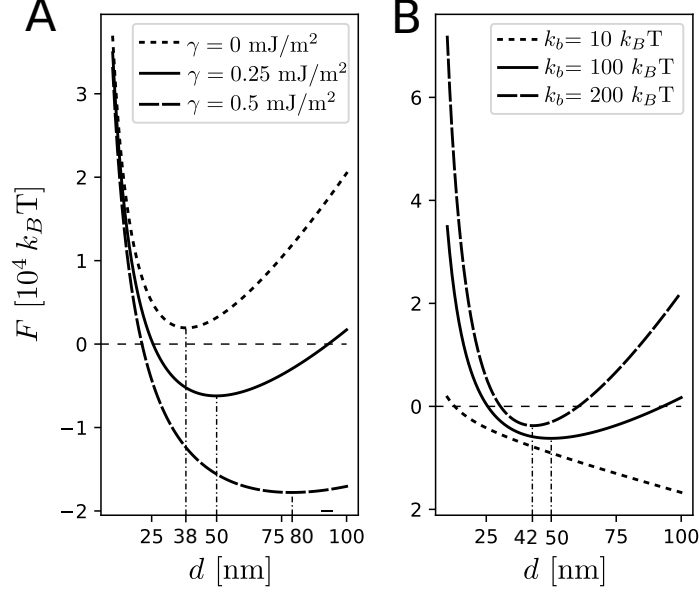


Figure 4: The effect of (A) surface energy density γ and (B) bending modulus of the membrane k_b on free energy minimum for $C_0 = 50 \mu\text{m}^{-1}$ and $l = 1000$ nm. Solid line correspond to Fig. 3C. Optimal diameter is depicted for each curve.

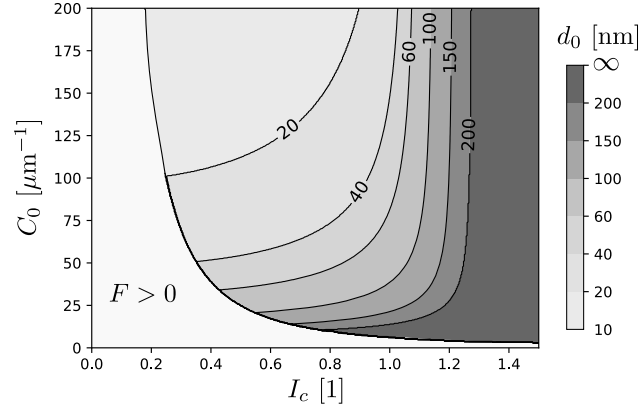


Figure 5: The optimal diameter as a function of interaction index $I_c = C_{\text{crit}}/C_0$.

4 Discussion

We have hypothesized, that the cell membrane mechanics determines optimal topology of titanium nanostructured surface. The optimal surface topology is defined as a geometry that forms membrane into minimum energy shape. Cell membrane free energy accounts for the cost of the bending energy and the gain in the adhesion energy. The model explains previous experimental studies providing ambiguous values of optimal diameter of TNTs for cell growth. Model simulation show that either small diameters as observed by Park et al, 2007 [16] (Fig. 3D) or larger diameters reported by Brammer et al, 2009 [26] (Fig. 3C) are feasible within certain range of parameters describing adhesion and bending energy.

Model analysis indicate that the spontaneous curvature relative to critical curvature (Eq. 5) determines existence of optimal surface topology given by optimal diameter d_0 . However, critical curvature value does not discriminate whether the cell is or is not attached to the surface. Therefore, we have defined a new dimensionless parameter describing the interactions between the cells and the nanostructured surface, the cell interaction index I_c (Eq. (6)). The cell interaction index shows, that a certain parameters range describing cell mechanics predispose the cell to form stable protrusions into nanostructured surface of specific topology. For example, it was reported that proliferation of vascular smooth muscle cells is higher on flat TiO_2 surface while the endothelial cells prefer TNT surface [41,42]. Experimental study

show that smooth muscle cells lose their affinity to TNTs after plasma treatment [42]. Plasma treatment is known to increase surface energy and therefore increase also C_{crit} and I_c . High I_c corresponds to minimum energy at flat surface in Fig. 5 in agreement with experiment. On the other hand, preference to curved nanostructured surface can be caused either by high bending modulus, low adhesion or high spontaneous curvature. The latter was reported to be high in endothelial cells [43]. The preference to small diameter TNT surface was also observed in cancer cells [2, 18] that generally have lower adhesion strength [44] and therefore low I_c in Fig. 5.

However, if the adhesion is too low or bending rigidity too high (I_c close to zero), the cell will not adhere to the surface (Fig. 5). For example, TNT surface decreases the adherence of all bacteria [45, 46]. Gram-positive bacteria is surrounded by a bacterial wall of stiff glycan strands cross-linked into lipid bilayer [47]. This composite structure considerably increases bending rigidity [48]. High bending rigidity implies low I_c and limited protrusion into TNT wall (Fig. 5). For bacteria, TNT surface has small contact area restricted to the terminal ends of nanotubes as protrusion formation is energetically unfavourable.

Previous studies on TNT bioactivity focus mostly on material properties like surface chemistry, crystallinity, nanotube size, or water contact angles. The current study supplements previous research by studying the adhesion from the perspective of the cell while the cell-substrate interactions are described by the binding energy (Eq. 1). As-synthesized TNT are an extension of the amorphous TiO_2 layer [5] and after heat treatment the crystallinity of TiO_2 is improved [45]. Titanium crystallinity (amorphous versus anatase structures) enhances mechanical strength and increases hydrophilicity, which might improve cell adhesion and proliferation [21, 49]. Our results indicate, that the high cell adhesion itself (higher I_c) is required for cell attachment, but not inevitable for having an optimal TNT diameter. The same holds for the water contact angle that is another measure of surface energy [11].

The model was intentionally kept simple for clarity. However, there are many other parameters and mechanisms that could be considered in description of cell-nanosurface interactions. The adherence is described by a single adhesion energy constant γ . The cell adhesion is a complex process facilitated by charged protein-mediators [30]. The adhesion of proteins is shown to be higher for larger diameter TNT that could further facilitate adhesion [50]. The increase in surface charge could enhance protein adhesion and promote osteoblast cell proliferation [51]. Spontaneous curvature of the membrane C_0 is one of the main investigated parameters within the current study (Figs. 3, 5). While the spontaneous curvature of lipid bilayer is mostly determined by its lipid composition, local spontaneous curvature is driven by trans-plasma-membrane or peripheral proteins [40]. Therefore, the spontaneous curvature may not be constant, but it is likely to change along protrusion. In addition, proteins not only generate curvature, but can also sense membrane curvature [52] and accumulate at curved membrane area [53]. Similarly, microgrid topography of TiO_2 stimulated hMSC adhesion and spreading area while nanotopography favoured hMSC motility, and osteogenic differentiation [54].

It is well accepted that the deformation of cell membrane, interacting with the attached cytoskeleton, affects cell proliferation and differentiation [37]. For cell adhesion, a complex network of transmembrane integrins and cytoplasmic proteins is of the utmost importance [55]. Extracellular components of integrins attach to extracellular matrix while their intracellular components are attached to F-actin through adapter proteins [56] and may directly affect cell nucleus shape [57]. Park et al, 2007 [16] proposed a hypothesis, that optimal diameter of nanotubes is determined by integrin size. The size of extracellular domain of integrins is about 10 to 12 nm [56] and thus close integrin packing results in optimal integrin activation. This hypothesis is supported by the measurements showing that the 15-20 nm spacing is optimal for cell adhesion, proliferation, migration, and differentiation [16, 19]. This theory was further implemented into the mathematical model of osteoblast adhesion [30]. The model well explains narrow window of optimal diameter observed by Park et al, 2009 [19] but cannot explain stability of larger diameters [8].

The integrins are also sensitive to the membrane mechanical state including the curvature [58]. It was shown, that higher concentration of integrins occurs at the neck of protrusive podosome-like structures if the substrate is porous [59]. Podosome neck corresponds to part III in Fig. 2. It is reasonable to assume, that the same shape of membrane within TNT will provide similar accumulation of integrins. It was proposed, that negative membrane curvature increases separation of integrin cytoplasmic tails, which is known to promote integrin activation [60]. Therefore we complement a hypothesis of Park et al, 2007 [16] by adding the role of membrane protrusions into TNTs. The nanostructured protrusion induces negative curvature in the neck (part III in Fig. 2). Area of negative curvature results in accumulation of integrins and their activation. Actin filaments transmit the focal adhesion signal to the nucleus activating nuclear mechanotransduction pathways [57]. Park et al, 2017 observed no focal contact formation for larger TNT diameters. According to Fig. 3D, no protrusion is formed ($F > 0$) and therefore no region of negative curvature enhancing focal contact exists. This theory is in agreement with molecular dynamics simulation showing that nanopore-induced membrane curvature increases bioactivity locally at the neck region [61].

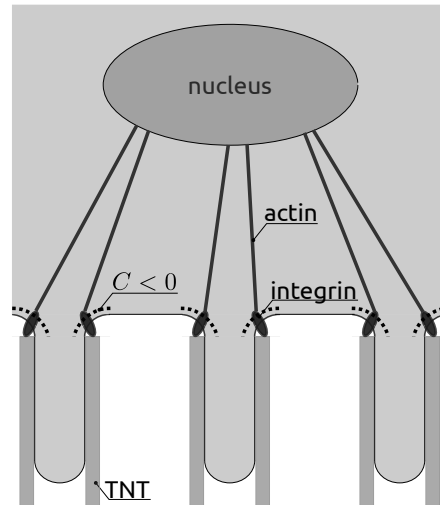


Figure 6: Mechanism of integrin activation at negative curvature area caused by cell membrane migration into TNT. Actin transmit the information on focal adhesion to nucleus.

5 Conclusions

The formation of membrane protrusions into TiO_2 nanotubes was assessed by means of cell membrane free energy. Dimensionless parameter, the cell interaction index I_c , was introduced to describe interplay between the cell membrane mechanics and the nanostructured surface topology. If I_c is close to zero, no membrane protrusions are formed and no cell adhesion occurs. For I_c greater than one, the cells prefer flat surface. For I_c approximately between zero and one, there exist an optimal diameter of TNT for given cell line. This study provides a theoretical basis explaining ambiguous results of experimental studies reporting wide range of suitable TNT diameters. It was proposed, that negative curvature region at the neck of membrane protrusion may result in integrin activation and subsequent cell proliferation. The results indicates a possibility to tune the topology of nanostructural material in a way to enhance proliferation and differentiation of one cell type that is mechanically compatible with given surface geometry while suppress the growth of other mechanically incompatible cells.

Funding

This research was funded by Czech grant agency grant number 16-14758S.

References

- [1] Liviu Feller, Yusuf Jadwat, Razia A.G. Khammissa, Robin Meyerov, Israel Schechter, and Johan Lemmer. Cellular responses evoked by different surface characteristics of intraosseous titanium implants. *Biomed Res. Int.*, 2015, 2015.
- [2] Roghayeh Imani, Doron Kabaso, Mateja Erdani Kreft, Ekaterina Gongadze, Samo Penic, Kristina Elersic, Andrej Kos, Peter Veranic, Robert Zorec, and Ales Iglic. Morphological alterations of T24 cells on flat and nanotubular TiO_2 surfaces. *Croat. Med. J.*, 53(6):577–85, 2012.
- [3] Julio C.M. Souza, Mariane B. Sordi, Miya Kanazawa, Sriram Ravindran, Bruno Henriques, Filipe S. Silva, Conrado Aparicio, and Lyndon F. Cooper. Nano-scale modification of titanium implant surfaces to enhance osseointegration. *Acta Biomater.*, 94:112–131, 2019.
- [4] Tolou Shokuhfar, Azhang Hamlekhan, Jen Yung Chang, Chang Kyoung Choi, Cortino Sukotjo, and Craig Friedrich. Biophysical evaluation of cells on nanotubular surfaces: The effects of atomic ordering and chemistry. *Int. J. Nanomedicine*, 9(1):3737–3748, 2014.
- [5] Daniel Martinez-Marquez, Karan Gulati, Christopher P. Carty, Rodney A. Stewart, and Sašo Ivanovski. Determining the relative importance of titania nanotubes characteristics on bone implant surface performance: A quality by design study with a fuzzy approach. *Mater. Sci. Eng. C*, 114(April), 2020.

- [6] Sepideh Minagar, Christopher C Berndt, James Wang, Elena Ivanova, and Cuie Wen. Author 's personal copy Acta Biomaterialia A review of the application of anodization for the fabrication of nanotubes on metal implant surfaces.
- [7] Tao Li, Karan Gulati, Na Wang, Zhenting Zhang, and Sašo Ivanovski. Understanding and augmenting the stability of therapeutic nanotubes on anodized titanium implants. *Mater. Sci. Eng. C*, 88(March):182–195, 2018.
- [8] Christine J Frandsen, Karla S Brammer, and Sungho Jin. Variations to the nanotube surface for bone regeneration. *Int. J. Biomater.*, 2013:513680, jan 2013.
- [9] Y. Q. Hao, S. J. Li, Y. L. Hao, Y. K. Zhao, and H. J. Ai. Effect of nanotube diameters on bioactivity of a multifunctional titanium alloy. *Appl. Surf. Sci.*, 268:44–51, 2013.
- [10] Fei Wei, Mengting Li, Ross Crawford, Yinghong Zhou, and Yin Xiao. Exosome-integrated titanium oxide nanotubes for targeted bone regeneration. *Acta Biomater.*, 86:480–492, 2019.
- [11] Azhang Hamlekhan, Arman Butt, Sweetu Patel, Dmitry Royhman, Christos Takoudis, Cortino Sukotjo, Judy Yuan, Gregory Jursich, Mathew T. Mathew, William Hendrickson, Amarjit Virdi, and Tolou Shokuhfar. Fabrication of anti-aging TiO₂ nanotubes on biomedical Ti alloys. *PLoS One*, 9(5), 2014.
- [12] K. Indira, U. Kamachi Mudali, T. Nishimura, and N. Rajendran. A Review on TiO₂ Nanotubes: Influence of Anodization Parameters, Formation Mechanism, Properties, Corrosion Behavior, and Biomedical Applications. *J. Bio- Tribo-Corrosion*, 1(4):1–22, 2015.
- [13] Maggie Paulose, Haripriya E. Prakasam, Oomman K. Varghese, Lily Peng, Ketul C. Papat, Gopal K. Mor, Tejal A. Desai, and Craig A. Grimes. TiO₂ Nanotube Arrays of 1000 μm Length by Anodization of Titanium Foil: Phenol Red Diffusion. *J. Phys. Chem. C*, 111(41):14992–14997, oct 2007.
- [14] Zhaoxiang Peng and Jiahua Ni. Surface properties and bioactivity of TiO₂ nanotube array prepared by two-step anodic oxidation for biomedical applications. *R. Soc. Open Sci.*, 6(4), 2019.
- [15] M Kulkarni, A Mazare, E Gongadze, Perutkova, V Kralj-Iglic, I Milošev, P Schmuki, A Igljč, and M Mozetič. Titanium nanostructures for biomedical applications. *Nanotechnology*, 26(6), 2015.
- [16] Jung Park, Sebastian Bauer, Klaus von der Mark, and Patrik Schmuki. Nanosize and vitality: TiO₂ nanotube diameter directs cell fate. *Nano Lett.*, 7(6):1686–91, jun 2007.
- [17] Sepideh Minagar, James Wang, Christopher C Berndt, Elena P Ivanova, and Cuie Wen. Cell response of anodized nanotubes on titanium and titanium alloys. *J. Biomed. Mater. Res. A*, 101(9):2726–39, sep 2013.
- [18] Ang Tian, Xiao Fei Qin, Anhua Wu, Hangzhou Zhang, Quan Xu, Deguang Xing, He Yang, Bo Qiu, Xiangxin Xue, Dongyong Zhang, and Chenbo Dong. Nanoscale TiO₂ nanotubes govern the biological behavior of human glioma and osteosarcoma cells. *Int. J. Nanomedicine*, 10:2423–2439, 2015.
- [19] Jung Park, Sebastian Bauer, Karl Andreas Schlegel, Friedrich W. Neukam, Klaus Der Von Mark, and Patrik Schmuki. TiO₂ nanotube surfaces: 15 nm - an optimal length scale of surface topography for cell adhesion and differentiation. *Small*, 5(6):666–671, 2009.
- [20] Wei Qiang Yu, Xing Quan Jiang, Fu Qiang Zhang, and Ling Xu. The effect of anatase TiO₂ nanotube layers on MC3T3-E1 preosteoblast adhesion, proliferation, and differentiation. *J. Biomed. Mater. Res. - Part A*, 94(4):1012–1022, 2010.
- [21] Yuliya Y Khrunyk, Sergey V Belikov, Mikhail V Tsurkan, Ivan V Vyalykh, Alexandr Y Markaryan, Maxim S Karabanalov, Artemii A Popov, and Marcin Wysokowski. Surface-dependent osteoblasts response to TiO₂ nanotubes of different crystallinity. *Nanomaterials*, 10(2):1–17, 2020.
- [22] Kakoli Das. TiO₂ nanotubes on Ti: Influence of nanoscale morphology on bone cell–materials interaction. *J. Biomed. . . .*, 90(1):225–37, jul 2009.
- [23] Seunghan Oh, Karla S Brammer, Y S Julie Li, Dayu Teng, Adam J Engler, Shu Chien, and Sungho Jin. Stem cell fate dictated solely by altered nanotube dimension. *Proc. Natl. Acad. Sci. U. S. A.*, 106(7):2130–5, feb 2009.
- [24] Seunghan Oh, Karla S Brammer, Y S Julie Li, Dayu Teng, Adam J Engler, Shu Chien, and Sungho Jin. Stem cell fate dictated solely by altered nanotube dimens. *PNAS*, 2008.
- [25] Mengyan Li, Mark J Mondrinos, Xuesi Chen, Milind R Gandhi, Frank K Ko, and Peter I Lelkes. Elastin Blends for Tissue Engineering Scaffolds. *J. Biomed. Mater. Res. Part A*, 79(4):963–73, 2006.
- [26] Karla S. Brammer, Seunghan Oh, Christine J. Cobb, Lars M. Bjursten, Henri van der Heyde, and Sungho Jin. Improved bone-forming functionality on diameter-controlled TiO₂ nanotube surface. *Acta Biomater.*, 5(8):3215–3223, 2009.

- [27] Elena Filova, Jaroslav Fojt, Marketa Kryslova, Hynek Moravec, Ludek Joska, and Lucie Bacakova. The diameter of nanotubes formed on Ti-6Al-4V alloy controls the adhesion and differentiation of Saos-2 cells. *Int. J. Nanomedicine*, 10:7145–7163, 2015.
- [28] Barbora Voltrova, Vojtech Hybasek, Veronika Blahnova, Josef Sepitka, Vera Lukasova, Karolina Vocetkova, Vera Sovkova, Roman Matejka, Jaroslav Fojt, Ludek Joska, Matej Daniel, and Eva Filova. Different diameters of titanium dioxide nanotubes modulate Saos-2 osteoblast-like cell adhesion and osteogenic differentiation and nanomechanical properties of the surface. *RSC Adv.*, 9(20):11341–11355, 2019.
- [29] Jung Park, Sebastian Bauer, Patrik Schmuki, and Klaus Von Der Mark. Narrow window in nanoscale dependent activation of endothelial cell growth and differentiation on TiO₂ nanotube surfaces. *Nano Lett.*, 9(9):3157–3164, 2009.
- [30] Ekaterina Gongadze, Doron Kabaso, Sebastian Bauer, Jung Park, Patrik Schmuki, and Ales Iglic. Adhesion of Osteoblasts to a Vertically Aligned TiO₂ Nanotube Surface. *Mini-Reviews Med. Chem.*, 13(2):194–200, 2013.
- [31] Dainelys Guadarrama Bello, Aurélien Fouillen, Antonella Badia, and Antonio Nanci. A nanoporous titanium surface promotes the maturation of focal adhesions and formation of filopodia with distinctive nanoscale protrusions by osteogenic cells. *Acta Biomater.*, 60:339–349, 2017.
- [32] Erich Sackmann and Ana Sunčana Smith. Physics of cell adhesion: Some lessons from cell-mimetic systems. *Soft Matter*, 10(11):1644–1659, 2014.
- [33] W Helfrich. Elastic properties of lipid bilayers: theory and possible experiments. *Zeitschrift für Naturforschung. Tl. C. Biochem. Biophys. Biol. Virol.*, 11(28):693–703, 1973.
- [34] Patricia Bassereau, Rui Jin, Tobias Baumgart, Markus Deserno, Rumiana Dimova, Vadim A. Frolov, Pavel V. Bashkirov, Helmut Grubmüller, Reinhard Jahn, H. Jelger Risselada, Ludger Johannes, Michael M. Kozlov, Reinhard Lipowsky, Thomas J. Pucadyil, Wade F. Zeno, Jeanne C. Stachowiak, Dimitrios Stamou, Artú Breuer, Line Lauritsen, Camille Simon, Cécile Sykes, Gregory A. Voth, and Thomas R. Weikl. The 2018 biomembrane curvature and remodeling roadmap. *J. Phys. D. Appl. Phys.*, 51(34), 2018.
- [35] Morgan Chabanon and Padmini Rangamani. Gaussian curvature directs the distribution of spontaneous curvature on bilayer membrane necks. *Soft Matter*, 14(12):2281–2294, 2018.
- [36] Adnan Morshed, Buddini Iroshika Karawdeniya, Y. M. Nuwan D.Y. Bandara, Min Jun Kim, and Prashanta Dutta. Mechanical characterization of vesicles and cells: A review. *Electrophoresis*, 41(7-8):449–470, 2020.
- [37] Bruno Pontes, Yareni Ayala, Anna Carolina C. Fonseca, Luciana F. Romão, Rachele F. Amaral, Leonardo T. Salgado, Flavia R. Lima, Marcos Farina, Nathan B. Viana, Vivaldo Moura-Neto, and H. Moysés Nussenzweig. Membrane Elastic Properties and Cell Function. *PLoS One*, 8(7):e67708, jul 2013.
- [38] Rudolf Winklbauer. Dynamic cell-cell adhesion mediated by pericellular matrix interaction - a hypothesis. *J. Cell Sci.*, 132(16), 2019.
- [39] Harvey T McMahon and Jennifer L Gallop. Membrane curvature and mechanisms of dynamic cell membrane remodelling. *Nature*, 438(7068):590–6, dec 2005.
- [40] Semen O. Yesylevskyy, Timothée Rivel, and Christophe Ramseyer. The influence of curvature on the properties of the plasma membrane. Insights from atomistic molecular dynamics simulations. *Sci. Rep.*, 7(1):1–13, 2017.
- [41] Lily Peng, Matthew L. Eltgroth, Thomas J. LaTempa, Craig A. Grimes, and Tejal A. Desai. The effect of TiO₂ nanotubes on endothelial function and smooth muscle proliferation. *Biomaterials*, 30(7):1268–1272, 2009.
- [42] Ita Junkar, Mukta Kulkarni, Metka Benčina, Janez Kovač, Katjuša Mrak-Poljšak, Katja Lakota, Snežna Sodini-Šemrl, Miran Mozetič, and Aleš Iglič. Titanium Dioxide Nanotube Arrays for Cardiovascular Stent Applications. *ACS Omega*, 5(13):7280–7289, 2020.
- [43] Geert W Schmid-Schönbein, Tadashi Kosawada, Richard Skalac, and Shu Chien. Membrane model of endothelial cells and leukocytes. A proposal for the origin of a cortical stress. *J. Biomech. Eng.*, 117(2):171–178, 1995.
- [44] Alexander Fuhrmann, Afsheen Banisadr, Pranjali Beri, Thea D Tlsty, and Adam J Engler. Metastatic State of Cancer Cells May Be Indicated by Adhesion Strength. *Biophys. J.*, 112(4):736–745, 2017.
- [45] Batur Ercan, Erik Taylor, Ece Alpaslan, and Thomas J Webster. Diameter of titanium nanotubes influences anti-bacterial efficacy. *Nanotechnology*, 22(29), 2011.
- [46] Sabrina D Puckett, Erik Taylor, Theresa Raimondo, and Thomas J Webster. The relationship between the nanostructure of titanium surfaces and bacterial attachment. *Biomaterials*, 31(4):706–713, 2010.
- [47] Christine E Harper and Christopher J Hernandez. Cell biomechanics and mechanobiology in bacteria: Challenges and opportunities. *APL Bioeng.*, 4(2):21501, 2020.

- [48] George K Auer and Douglas B Weibel. Bacterial Cell Mechanics. *Biochemistry*, 56(29):3710–3724, 2017.
- [49] A Mazare, M Dilea, D Ionita, I Titorencu, V Trusca, and E Vasile. Changing bioperformance of TiO₂ amorphous nanotubes as an effect of inducing crystallinity. *Bioelectrochemistry*, 87:124–131, 2012.
- [50] Ekaterina Gongadze, Šarka Perutková, Veronika Kralj-Iglič, Ursula van Rienen, Ulrich Beck, Aleš Iglič, and Doron Kabaso. Electromechanical Basis for the Interaction Between Osteoblasts and Negatively Charged Titanium Surface. pages 199–221. 2011.
- [51] Amit Bandyopadhyay, Anish Shivaram, Indranath Mitra, and Susmita Bose. Electrically polarized TiO₂ nanotubes on Ti implants to enhance early-stage osseointegration. *Acta Biomater.*, 96:686–693, 2019.
- [52] Artù Breuer, Line Lauritsen, Elena Bertseva, Ivana Vonkova, and Dimitrios Stamou. Quantitative investigation of negative membrane curvature sensing and generation by I-BARs in filopodia of living cells. *Soft Matter*, 15(48):9829–9839, 2019.
- [53] H Strahl, S Ronneau, B Solana González, D Klutsch, C Schaffner-Barbero, and L W Hamoen. Transmembrane protein sorting driven by membrane curvature. *Nat. Commun.*, 6, 2015.
- [54] Peng Chen, Toshihiro Aso, Ryuichiro Sasaki, Maki Ashida, Yusuke Tsutsumi, Hisashi Doi, and Takao Hanawa. Adhesion and differentiation behaviors of mesenchymal stem cells on titanium with micrometer and nanometer-scale grid patterns produced by femtosecond laser irradiation. *J. Biomed. Mater. Res. Part A*, 106(10):2735–2743, oct 2018.
- [55] Feng Luo, Guang Hong, Hiroyuki Matsui, Kosei Endo, Qianbing Wan, and Keiichi Sasaki. Initial osteoblast adhesion and subsequent differentiation on zirconia surfaces are regulated by integrins and heparin-sensitive molecule. *Int. J. Nanomedicine*, 13:7657–7667, 2018.
- [56] Pakorn Kanchanawong, Gleb Shtengel, Ana M Pasapera, Ericka B Ramko, Michael W Davidson, Harald F Hess, and Clare M Waterman. Nanoscale architecture of integrin-based cell adhesions. *Nature*, 468(7323):580–584, nov 2010.
- [57] Karine Anselme, Nayana Tusamda Wakhloo, Pablo Rougerie, and Laurent Pieuchot. Role of the Nucleus as a Sensor of Cell Environment Topography. *Adv. Heal. Mater.*, 7(8):1–17, 2018.
- [58] Jenny Z Kechagia, Johanna Ivaska, and Pere Roca-Cusachs. Integrins as biomechanical sensors of the microenvironment. *Nat. Rev. Mol. Cell Biol.*, 20(8):457–473, 2019.
- [59] Maksim V Baranov, Ter Martinter Beest, Inge Reinieren-Beeren, Alessandra Cambi, Carl G Figdor, and Geert Van Den Bogaart. Podosomes of dendritic cells facilitate antigen sampling. *J. Cell Sci.*, 127(5):1052–1064, 2014.
- [60] Xenia Meshik, Patrick R O’Neill, and N Gautam. Physical Plasma Membrane Perturbation Using Subcellular Optogenetics Drives Integrin-Activated Cell Migration. *ACS Synth. Biol.*, 8(3):498–510, mar 2019.
- [61] Alexis Belessiotis-Richards, Stuart G. Higgins, Ben Butterworth, Molly M. Stevens, and Alfredo Alexander-Katz. Single-Nanometer Changes in Nanopore Geometry Influence Curvature, Local Properties, and Protein Localization in Membrane Simulations. *Nano Lett.*, 19(7):4770–4778, 2019.
- [62] David Boal. *Mechanics of the Cell*. Cambridge University Press, Cambridge, 2002.

A Bending energy of membrane protrusion

Energy of membrane forming tubular structure depends on curvature of individual parts depicted in Fig. 2. According to the curvature, the membrane protrusion could be divided into three parts (Fig. 2). The first segment correspond to the hemispherical cup, where both principal curvatures equals to $2/d$ and the energy of the first segment could be expressed as

$$F_{bI} = k_b \pi \left(4 - 2 d C_0 + \left(\frac{d C_0}{2} \right)^2 \right) \quad (7)$$

The free energy of the central cylindrical part (Fig. 2, II) is determined by its length l while the first and the second membrane curvature are $2/d$ and 0, respectively.

$$F_{bII} = \frac{1}{2} k_b \pi l \left(\frac{4}{d} - 4 C_0 + C_0^2 d \right) \quad (8)$$

The last part presents a neck, that connect a protrusion to the cell. The neck is modeled as axisymmetrical structure with one radius of curvature equal to ρ (Fig. 2, III). The first curvature is negative as the membrane bends outwards, $C_1 = -1/\rho$. The second radius of curvature depends on the distance from axis of symmetry and could be expressed as $C_2 = \sin(\varphi)/(d/2 + \rho(1 - \sin(\varphi)))$ [62] where φ is defined in Fig. 2. For the sake of simplicity, we further assume that the radius ρ equals to $d/2$. The energy could be expressed after integration of Eq. (2) over the part III as

$$F_{bIII} = \frac{1}{2} k_b \pi d \left(\frac{\pi C_0^2 d}{2} - \frac{C_0^2 d}{2} + \frac{16 \pi}{3^{\frac{3}{2}} d} - \frac{8}{d} + 2 \pi C_0 - 4 C_0 \right) \quad (9)$$

The total energy can be expressed as a sum of Eq. (1) and Eqs. (7)–(9).